The Arabidopsis SMO2, a homologue of yeast TRM112, modulates progression of cell division during organ growth

Zhubing Hu[1,2], Zhixiang Qin[1], Min Wang[1,2], Chongyi Xu[1], Guanping Feng[1,2], Jing Liu[1,2], Zheng Meng[1] and Yuxin Hu[1,3,*]

[1]*Key Laboratory of Photosynthesis and Environmental Molecular Physiology, Institute of Botany, Chinese Academy of Sciences, Beijing 100093, China,*
[2]*Graduate School of Chinese Academy of Sciences, Beijing, China, and*
[3]*National Center for Plant Gene Research, Beijing, China*

SUMMARY

Cell proliferation is integrated into developmental progression in multicellular organisms, including plants, and the regulation of cell division is of pivotal importance for plant growth and development. Here, we report the identification of an Arabidopsis *SMALL ORGAN 2* (*SMO2*) gene that functions in regulation of the progression of cell division during organ growth. The *smo2* knockout mutant displays reduced size of aerial organs and shortened roots, due to the decreased number of cells in these organs. Further analyses reveal that disruption of *SMO2* does not alter the developmental timing but reduces the rate of cell production during leaf and root growth. Moreover, *smo2* plants exhibit a constitutive activation of cell cycle-related genes and over-accumulation of cells expressing CYCB1;1:β-glucuronidase (CYCB1;1:GUS) during organogenesis, suggesting that *smo2* has a defect in G_2–M phase progression in the cell cycle. *SMO2* encodes a functional homologue of yeast TRM112, a plurifunctional component involved in a few cellular events, including tRNA and protein methylation. In addition, the mutation of *SMO2* does not appear to affect endoreduplication in Arabidopsis leaf cells. Taken together we postulate that Arabidopsis SMO2 is a conserved yeast TRM112 homologue and SMO2-mediated cellular events are required for proper progression of cell division in plant growth and development.

Keywords: *smo2*, TRM112, cell division, organ growth, *Arabidopsis thaliana*.

INTRODUCTION

Plant morphogenesis is largely post-embryonic, and new organs, including leaf, stem and flower, originate from meristem, followed by growth up to their specific sizes. Cell division, differentiation and expansion are pivotal processes necessary for organogenesis (Beemster *et al.*, 2003; Tsukaya, 2003, 2006, 2008; De Veylder *et al.*, 2007). Considerable advances have been made in recent years in understanding the control of cell division at the cellular level, and the basic molecular machinery driven by cyclin/cyclin-dependent kinase (CDK) complexes has been defined in model organisms, including animals and plants (Dewitte and Murray, 2003; Malumbres, 2005; Inzé and De Veylder, 2006; Gutierrez, 2009). However, the regulation of cell division during development is not well understood, partly because of the complexity of its tight coordination with cell differentiation/expansion and integration into developmental progression (Mizukami, 2001; Tsukaya, 2003, 2006, 2008; Ingram and Waites, 2006).

In plants, iterative cell divisions are essential for the maintenance of apical meristems and the growth of organs (Dewitte and Murray, 2003; Inzé and De Veylder, 2006; Gutierrez, 2009). In Arabidopsis, disruption of some cell cycle-related genes, such as *CYCD3* or *CDKB2*, leads to a defect in both meristem and organ development (Dewitte *et al.*, 2007; Andersen *et al.*, 2008), while disturbance of some other genes often alters organ growth and plant architecture. For example, mutation or misexpression of Arabidopsis genes such as *E2Fa* and *DPa*, *E2FC*, *RBR* or *CDKF;1*, inhibits the growth of aerial organs and thus reduces their final sizes (De Veylder *et al.*, 2002; Desvoyes *et al.*, 2006; del Pozo *et al.*, 2006; Takatsuka *et al.*, 2009). Overexpression of CDK inhibitors (KRPs) or the antiphosphatase PAS2, which modulates cyclin-dependent kinase A (CDKA) activity, impedes cell division and results in a stunted-plant phenotype with smaller organs (Wang *et al.*,

2000; De Veylder *et al.*, 2001; Da Costa *et al.*, 2006). In addition, recent studies on the control of plant organ size suggest that the duration of cell proliferation during organogenesis is a major factor in determining the overall size of plant organs (Anastasiou and Lenhard, 2007; Gonzalez *et al.*, 2009; Krizek, 2009).

As a fundamental biological process, cell division in plants is known to be modulated by a variety of developmental and environmental cues, such as plant hormones and light, at either cellular or whole plant levels (Beemster *et al.*, 2003; del Pozo *et al.*, 2005; Dohmann *et al.*, 2008; Achard *et al.*, 2009; Ubeda-Tomás *et al.*, 2009). On the other hand, most intrinsic cellular events may also impinge on the progression of cell division and thus affect plant growth and development. For instance, loss of function of Arabidopsis FASCIATA1 (FAS1), a chromatin assembly factor subunit, blocks mitotic progression in G_2–M phase, leading to irregular cellular organization in the apical meristems and the inhibition of organ growth (Kaya *et al.*, 2001; Ramirez-Parra and Gutierrez, 2007). Similar phenotypes have been reported in the Arabidopsis mutants of TEBICHI, a homologue of *Drosophila* and mammalian DNA polymerase θ involved in DNA repair (Inagaki *et al.*, 2006), and of HOBBIT (HBT), a CDC27 subunit of an anaphase-promoting complex (APC/C) (Willemsen *et al.*, 1998; Blilou *et al.*, 2002; Pérez-Pérez *et al.*, 2008). A recent study also revealed that disruption of Arabidopsis *HISTONE MONOUBIQUITINATION1* (*HUB1*) inhibits primary root and leaf growth, due to the misexpression of cell cycle genes in the G_2–M transition and a prolonged cell cycle duration (Fleury *et al.*, 2007), suggesting that histone modification is involved in regulation of the progression of cell division in plants.

TRM112 has been initially identified as a plurifunctional cofactor of methyltransferases involved in both tRNA and protein methylation in yeast (Purushothaman *et al.*, 2005; Heurgué-Hamard *et al.*, 2006). Biochemical analysis indicates that TRM112 is a subunit of both TRM11 and TRM9, two tRNA methyltransferases necessary for the formation of 2-methylguanosine at position 10 and modification of anticodons at the wobble uridine (U34) position, respectively (Purushothaman *et al.*, 2005; Studte *et al.*, 2008). TRM112 was further found to be a cofactor of eukaryotic release factor 1 (eRF1) methyltransferase (Heurgué-Hamard *et al.*, 2006), and might also interact with LYS9, a saccharopine dehydrogenase, and other proteins (Krogan *et al.*, 2006; Studte *et al.*, 2008; Yu *et al.*, 2008), implying that TRM112 possibly has a function in modification or regulation of a few other cellular processes in yeast. Recent biochemical study demonstrates that a human homologue of yeast TRM112 can interact with the HemK2α, a catalytic subunit of eRF1 methyltransferase, to methylate eRF1 *in vitro* (Figaro *et al.*, 2008), suggesting that TRM112 might be functionally conserved in multicellular organisms.

Here, we characterize an Arabidopsis *small organ 2* (*smo2*) mutant, in which cell proliferation is inhibited during growth of both aerial organs and root. We show that SMO2 is a functional homologue of *Saccharomyces cerevisiae* TRM112, and provide evidence that disruption of *SMO2* mainly inhibits the G_2–M phase progression during organogenesis. Our analyses demonstrate that Arabidopsis SMO2 retains the function of yeast TRM112 and is required for proper progression of cell division during organ growth.

RESULTS

Organ growth defects in *smo2*

To gain insight into how cell proliferation and/or cell expansion is controlled during organogenesis, we generated a transgenic Arabidopsis population with T-DNA activation-tagging, and screened the mutants that exhibited enhanced or inhibited growth of aerial organs. *small organ 2* (*smo2*) was initially isolated for its dramatic reduction in leaf size (Figure 1a). Detailed quantification showed that the blade area of the fully expanded fifth leaves in *smo2* only reached to about 40% of that in the wild type (WT) (Figure 1c). An apparent size reduction was further observed in all aerial organs in *smo2*, including cotyledon, hypocotyl, inflorescent stem, floral organs and fruits (siliques) (Figure 1d, Table 1), and consequently plant height in *smo2* decreased (Table 1). Furthermore, the growth of primary
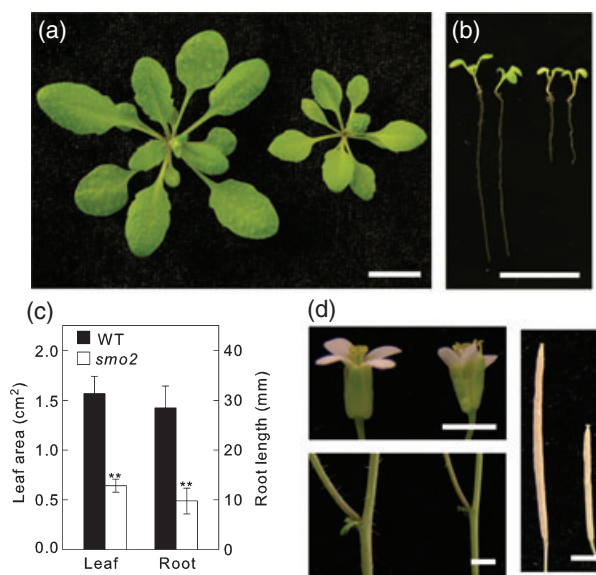
Figure 1 Organ growth is retarded in *smo2*.
(a, b) Morphology of Columbia-0 wild type (WT) (left) and *smo2* (right) plants. Four-week-old plants in (a) and 8-day-old seedlings in (b). Scale bars: 10 mm.
(c) The average area of fully expanded fifth leaves and primary root length of 8-day-old seedlings in WT and *smo2*. All the data were from at least 10 plants of each genotype and shown as average volumes ± SD; Student's *t*-test, **$P < 0.01$.
(d) Phenotype of flower, inflorescence stem, and silique of WT (left) and *smo2* (right). Scale bars: 2 mm.

Table 1 Phenotypic characterization of *smo2*. Fifty-day-old plants were used for measurement of plant heights and silique lengths, and flowering time is shown as the days from seed germination to first flower emergence. The cotyledon areas were measured with 20-day-old seedlings, and hypocotyl lengths were with 5-day-old seedlings grown in the dark. Data are shown as an average ± SD

Measurements	Wild type	*smo2*
Plant height (cm)	29.1 ± 1.4 (*n* = 8)	25.9 ± 1.2 (*n* = 8)
Silique length (mm)	13.2 ± 0.7 (*n* = 15)	7.9 ± 0.9 (*n* = 15)
Hypocotyl length (mm)	17.0 ± 0.7 (*n* = 20)	11.8 ± 2.5 (*n* = 20)
Flowering time (days)	26.2 ± 1.2 (*n* = 16)	25.8 ± 3.8 (*n* = 16)
Cotyledon area (mm^2)	7.9 ± 0.5 (*n* = 30)	5.2 ± 0.6 (*n* = 30)

roots in *smo2* seedlings was also found to be inhibited (Figure 1b), and the primary root length of 8-day-old seedlings of *smo2* was only 35% of that of the WT (Figure 1c). These observations indicate that the mutation of *SMO2* greatly impedes the growth of both aerial organs and root in Arabidopsis.

The organ growth defect in *smo2* is due to retarded cell proliferation

During organogenesis, cell proliferation and expansion/elongation are responsible for growth of an organ, and leaf and root have been found to be good models for studying organ development (Scheres and Wolkenfelt, 1998; Tsukaya, 2003, 2008). To understand the cellular basis of the reduction of organ size in *smo2*, cell proliferation and expansion in the leaf and root were further investigated. We first compared the leaf palisade cells, whose sizes contribute most to the final size of a leaf, between *smo2* and WT. As shown in Figure 2(a) and (b), in contrast to the dramatically reduced leaf size, the palisade cells of the fully expanded fifth leaf in *smo2* were found to be significantly enlarged. The estimated number of palisade cells per fifth leaf in *smo2* was only about 21% of that in the WT (Figure 2d). These observations imply that it is the defect in cell proliferation rather than cell expansion that accounts for the smaller leaf phenotype in *smo2*, and compensatory cell enlargement has occurred during *smo2* leaf growth and development.

We then compared the meristem and mature zones of the primary root between *smo2* and WT. Although cellular organization and cell size in the root meristem (RM) seemed to be similar between two genotypes (Figure 2c), the RM size and the number of meristematic cells in RM were apparently reduced in *smo2*, the number of meristematic cells in *smo2* RM being about 60% of that in WT RM (Figure 2c,d). However, in the mature zone of the root, the cortex cell length remained almost unchanged between WT (166 ± 10 μm) and *smo2* (169 ± 10 μm). Since RM size and cortex cell length in the mature zone reflect the status of cell division and cell elongation during root growth (Beemster and Baskin, 1998; Baskin, 2000; Ivanov *et al.*, 2002), our observation demonstrates that the mutation of *SMO2* affects
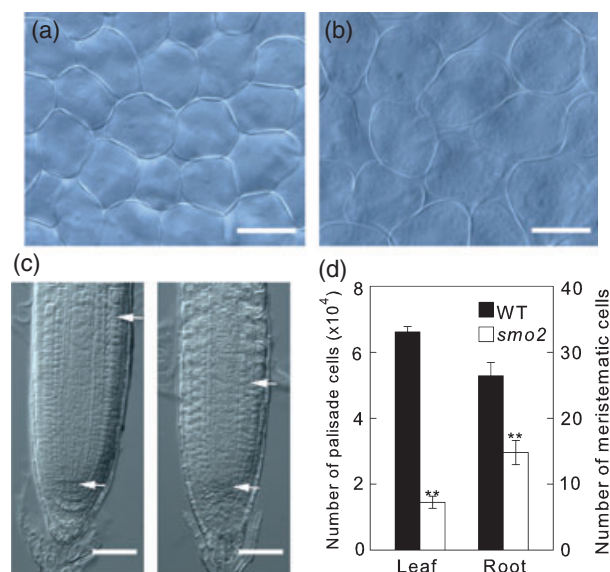
Figure 2. Anatomical characterization of *smo2* leaves and roots.
(a, b) The palisade cells of the fully expanded fifth leaf in wild type (WT) (a) and *smo2* plants (b). Scale bar: 50 μm.
(c) The root meristem (RM) image of 8-day-old seedlings of WT (left) and *smo2* plants (right). The top arrowhead indicates the transition zone between meristem and elongation-differentiation zone, and the bottom one marks the quiescent centre of the RM. Scale bar: 50 μm.
(d) The estimated palisade cell number per leaf and the cortex cell number of RM in WT and *smo2* plants. Five cleared blades of fully expanded fifth leaves from each genotype were used for measurement of the leaf area and determination of the palisade cell number per leaf under a microscope. At least 10 cleared roots from each genotype were counted for the cortex cell number in the RM. Data are shown as average values ± SD; Student's *t*-test, **P < 0.01.

cell proliferation rather than cell elongation during root development.

smo2 reduces the rate of cell production during leaf and root growth

In plants, the growth of an organ by cell proliferation is determined by the rate of cell production and developmental timing. To further examine the effect of *SMO2* on cell proliferation, we first compared the growth kinematics and rates of abaxial epidermal cell division of first leaves between *smo2* and WT. After initiation, the leaf blades expanded exponentially until 8 days in both WT and *smo2*, after which the leaf growth rate in *smo2* appeared to decrease much more than that in WT, and then blade growth ceased from the 13th day after initiation in both genotypes (Figure 3a). These observations imply that *smo2* does not affect the developmental timing of a leaf. In contrast to the dynamics of the leaf area in the two genotypes, epidermal cell number per leaf primordium seemed similar for the first 2 days, but the number differences per leaf then became significant since day 3 between WT and *smo2*, in which the cell numbers in *smo2* increased apparently more slowly than those in the WT (Figure 3b), suggesting that cell division is inhibited
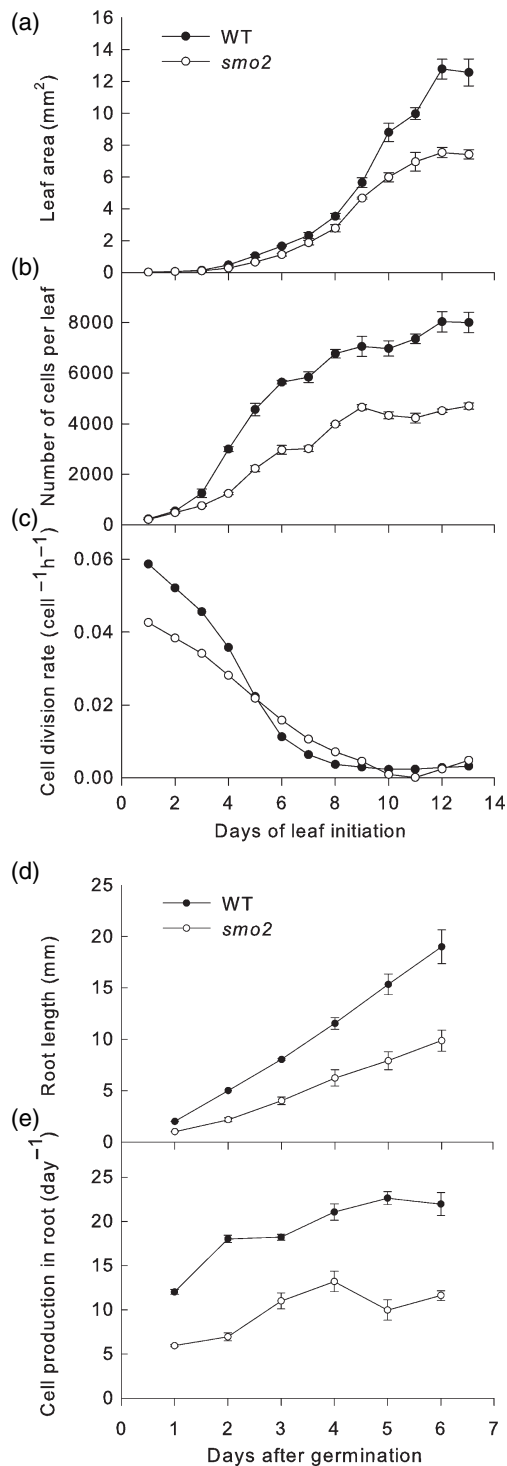
Figure 3. Growth kinematics and cell production analysis of *smo2* leaf and root.
(a) Average blade area of first leaves.
(b) Average epidermal cell number on the abaxial side of first leaves.
(c) Rate of cell division of epidermal cells on the abaxial side of first leaves.
(d) Average primary root length.
(e) Rate of cortex cell production in primary roots.
At least four blades of first leaves and eight primary roots from each genotype were assayed for their growth and cell production at each time point indicated. Data are shown as average values ± SE.

and compensatory cell expansion has occurred in *smo2* when a leaf undergoes growth by cell proliferation. To shed more light on the reduction in cell number in *smo2* leaf, we compared the rate of epidermal cell division between the two genotypes, and found that the rate of division of WT epidermal cells was indeed much higher than that of *smo2* ones at early stages; nevertheless, cell division in both WT and *smo2* blades then ceased almost at the same developmental time (Figure 3c), indicating that *smo2* does not affect the duration of cell division during leaf growth. Furthermore, the rate of production of cortex cell in *smo2* primary roots was also found to be constantly lower than that in WT after germination, consistent with the indeterminate manner of growth of primary roots at this developmental stage (Figure 3d,e). Taken together, we conclude that the mutation of *SMO2* reduces the rate of cell production during leaf and root growth.

smo2 has a defect in G_2–M phase progression

Because the rate of cell production is reduced in *smo2* leaf and root, we speculated that *smo2* might have a defect in progression of cell division. To test this, we first examined the expression of five cell cycle checkpoint-related genes in WT and *smo2*, including *CYCD3;1*, *HISTONE H4*, *CYCA1;1*, *CYCB2;3* and *CYCB1;1*, by real-time quantitative reverse-transcriptional polymerase chain reaction (qRT-PCR), and found that the expression of all these genes was elevated in the *smo2* mutant, among which the *CYCB1;1* transcripts in *smo2* reached a level of approximately 3.8-fold that in WT (Figure 4a), implying that the cell cycle in *smo2* is indeed disturbed.

To further substantiate the role of *SMO2* in cell cycle progression, we introduced a *pCYCB1;1:Dbox-GUS* construct into *smo2*. The CYCB1;1:GUS reporter marks a state of cells from G_2 to M phase progression, allowing us to visualize these cells at G_2–M phases (Colón-Carmona *et al.*, 1999). As shown in Figure 4(b) and (c), the number of cells expressing CYCB1;1:GUS in *smo2* RM was obviously more than that in WT RM, and the most dramatic accumulation of CYCB1;1:GUS protein was observed in *smo2* leaf primordia and juvenile leaves whose cells were undergoing cell proliferation, though basipetal gradients of GUS expression still existed in young leaves. Since *CYCB1;1* promoter is activated in G_2 phase and Dbox-GUS protein is degraded at metaphase (Colón-Carmona *et al.*, 1999; Criqui *et al.*, 2001), these observations, together with the highest up-regulated expression of *CYCB1;1* (Figure 4a) and decreased cell production in *smo2* leaf and root development (Figure 3), suggest that disruption of *SMO2* mainly delays or arrests cell cycle progression in the G_2 or M phase during organ growth.

Molecular cloning and expression of *SMO2*

Since *smo2* was isolated from a T-DNA mutagenesis population, we backcrossed *smo2* with the WT and examined F_1
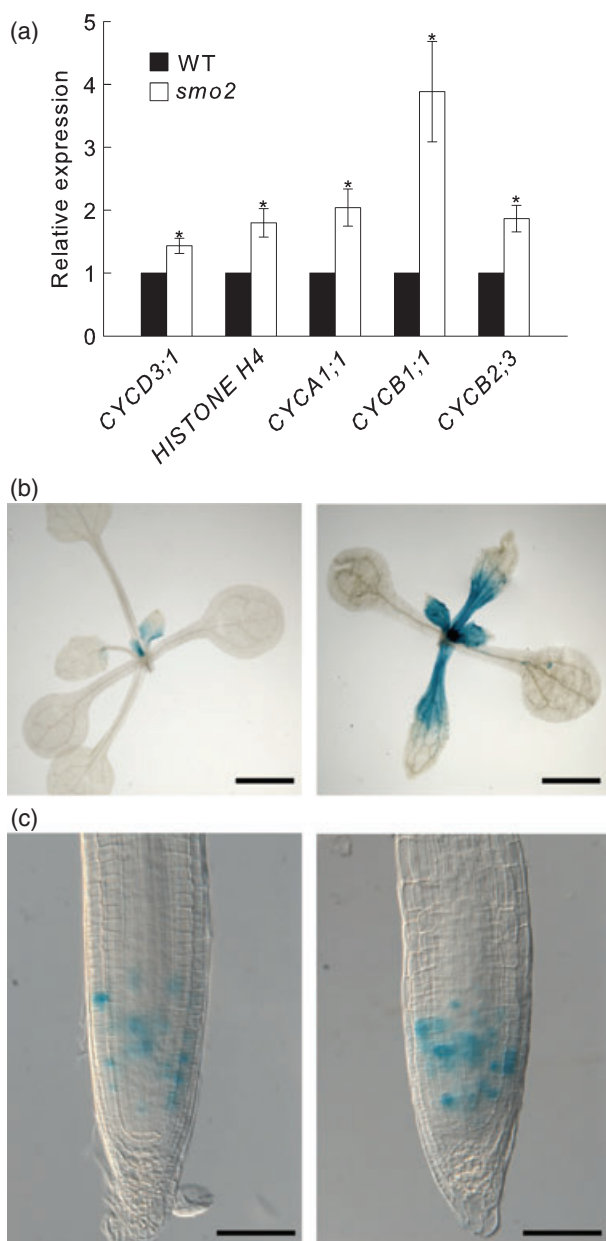
Figure 4. The expression of cell cycle-related genes in *smo2*.
(a) Expression levels of some cell cycle-related genes in wild type (WT) and *smo2*. Data were collected from the real-time quantitative RT-PCR analysis and are shown as averages ± SE from triplicate repeats and three biological replicates; Student's *t*-test, *$P < 0.05$.
(b) CYCB1;1-GUS expression in the leaf primordia and developing leaves of WT (left) and *smo2* (right). Twelve-day-old seedlings were assayed for the GUS activity. Scale bars: 2 mm.
(c) CYCB1;1-GUS staining in WT (left) and *smo2* (right) root meristem (RM) zones. Scale bars: 100 μm.

and F_2 progeny to understand the genetic nature of the mutation. All F_1 plants showed the WT phenotype, and F_2 plants displayed a segregation of WT:*smo2* as 3:1 (375:123, $P > 0.75$), demonstrating that *smo2* is a single-gene recessive mutant. Meanwhile, antibiotic resistance analysis of F_2

plants revealed that *smo2* contained a single T-DNA insertion in its genome (resistant:sensitive = 370:128) and the T-DNA insertion was co-segregated with *smo2* phenotype, suggesting that *smo2* is most likely caused by the T-DNA insertion event.
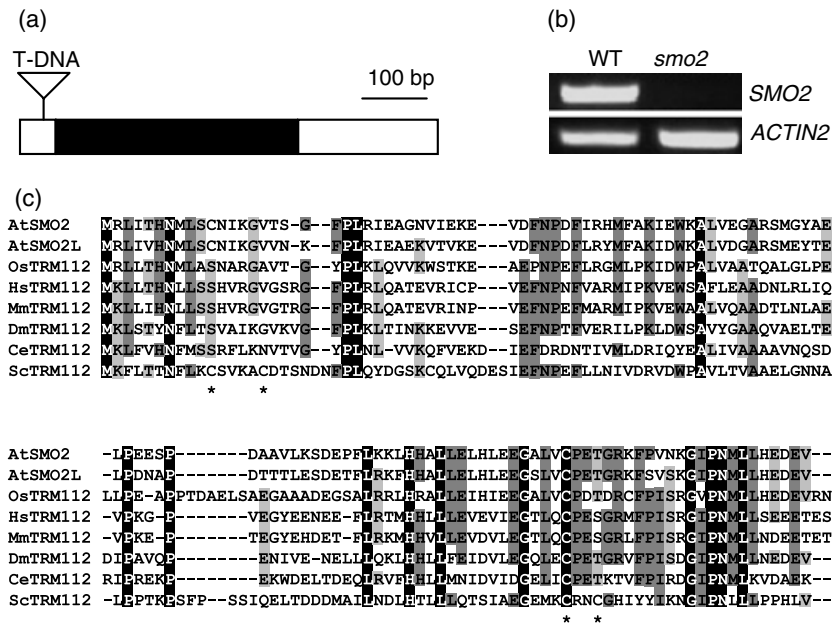
We then identified the genomic sequence flanking T-DNA by thermal asymmetric interlaced PCR (TAIL-PCR) (Liu *et al.*, 1995), and found that a T-DNA fragment was inserted at the 5′-untranslated region of *At1g22270*, 28 bp upstream of the start code ATG (Figure 5a). No transcript of *At1g22270* was detected in *smo2* plants by RT-PCR analysis (Figure 5b). To verify whether *At1g22270* is *SMO2*, a molecular complementation experiment was carried out by introducing a 2.5-kb WT genomic DNA fragment from the promoter to the 3′-untranslated region of *At1g22270* into *smo2*, and almost all transgenic *smo2* plants exhibited the WT morphology (Figure S1a in Supporting Information). We therefore conclude that the phenotypic change in *smo2* is caused by the disruption of *At1g22270*.

To determine the expression pattern of *SMO2*, we generated transgenic plants expressing a *pSMO2:GUS* fusion gene and examined GUS activities in seedlings and developing organs. As shown in Figure 6, strong GUS staining was observed in shoot and root meristem regions as well as in leaf and lateral root primordia, and a moderate level of GUS expression was detected in the cotyledon vascular bundles and root pericycles. In flowers, a high level of expression was mainly seen in young siliques (Figure 6e). The tissue-specific expression of *SMO2* is consistent with the role of *SMO2* in the regulation of cell division during organogenesis.

SMO2 encodes a small protein of 124 amino acids. In the Arabidopsis genome, there is another putative gene (*At1g78190*) that encodes a protein sharing ∼78% amino acid identity to SMO2, which is temporarily named SMO2-LIKE (SMO2L) (Figure 5c). However, the expression of *SMO2L* was only detected in anthers (Figure S1b), which was quite different from that of *SMO2* (Figure 6). Introduction of a construct of *pSMO2:SMO2L* into *smo2* failed to complement the organ growth defects in *smo2* (Figure S1a), suggesting that *SMO2L* and *SMO2* may have functionally diverged in Arabidopsis.

SMO2 encodes a functional homologue of yeast TRM112

A BLAST search in GenBank revealed that SMO2 shared amino acid similarity to yeast TRM112, a putative zinc-finger protein identified initially as a functional component of methyltransferases (Purushothaman *et al.*, 2005; Heurgué-Hamard *et al.*, 2006). SMO2 homologues were then found in the genomes of all model eukaryotic organisms, such as rice (*Oryza sativa*), human (*Homo sapiens*), mouse (*Mus musculus*), fruit fly (*Drosophila melanogaster*) and worm (*Caenorhabditis elegans*). Sequence alignment analysis showed that Arabidopsis SMO2 had 28–53% amino acid

(a)

T-DNA

100 bp

(b)

WT   *smo2*

SMO2

ACTIN2

(c)

```
AtSMO2   MRLITHNMLSCNIKGVTS-G--FPLRIEAGNVIEKE---VDFNPDFIRHMFAKIEWKALVEGARSMGYAE
AtSMO2L  MRLIVHNMLSCNIKGVVN-K--FPLRIEAEKVTVKE---VDFNPDFLRYMFAKIDWKALVDGARSMEYTE
OsTRM112 MRLLTHNMLASNARGAVT-G--YPLKLQVVKWSTKE---AEPNPEFLRGMLPKIDWPALVAATQALGLPE
HsTRM112 MKLLTHNLLSSHVRGVGSRG--FPLRLQATEVRICP---VEFNPNFVARMIPKVEWSAFLEAADNLRLIQ
MmTRM112 MKLLIHNLLSSHVRGVGTRG--FPLRLQATEVRINP---VEFNPEFMARMIPKVEWAALVQAADTLNLAE
DmTRM112 MKLSTYNFLTSVAIKGVKVG--FPLKLTINKKEVVE---SEFNPTFVERILPKLDWSAVYGAAQVAELTE
CeTRM112 MKLFVHNFMSSRFLKNVTVG--YPLNL-VVKQFVEKD---IEFDRDNTIVMLDRIQYEALIVAAAAVNQSD
ScTRM112 MKFLTTNFLKCSVKACDTSNDNFPLQYDGSKCQLVQDESIEFNPEFLLNIVDRVDWPAVLTVAAELGNNA
                    *       *                                    *    *
```

```
AtSMO2   -LEEESE-------DAAVLKSDEPFLKKLHADLELHLEEGALVCPETGRKFPVNKGIPNMILHEDEV--
AtSMO2L  -LEDNAE-------DTTTLESDETFLRKFHADLELHLEEGSLVCPETGRKFSVSKGIPNMILHEDEV--
OsTRM112 LLEE-AEPTDAELSAEGAAADEGSALRRLHRALLELHIEEGALVCPDTDRCFPISRGVPNMILHEDEVRN
HsTRM112 -VEKG-E-------VEGYEENEE-FLRTMAHLILEVEVIEGTLQCPESGRMFPISRGIPNMILSEEETES
MmTRM112 -VEKE-E-------TEGYEHDET-FLRKMRHVLLEVDVLEGTLQCPESGRLFPISRGIPNMILNDEETET
DmTRM112 DIEAVQE--------ENIVE-NELLIQKLRHLIFEIDVLEGQLECPETGRVFPISDGIPNMILNEDEV--
CeTRM112 RIEREKE--------EKWDELTDEQIRVFLHLDMNIDVIDGELICPETKTVFPIRDGIPNMIKVDAEK--
ScTRM112 -LEPTKESFP--SSIQELTDDDMAILNDLETLILLQTSIAEGEMKCRNCGHIYYIKNGIPNILLPPHLV--
                                   *   *                       *   *
```

Figure 5. Molecular cloning of *SMO2*.
(a) Schematic representation of the *SMO2* locus. The coding region of *SMO2* (*At1g22270*) is indicated as a black rectangle and untranslated regions (UTRs) as white rectangles. The T-DNA (triangle) was inserted at the 5′ UTR of *SMO2*, 28 bp upstream of ATG.
(b) The RT-PCR analysis of *SMO2* expression in wild type (WT) and *smo2* plants.
(c) Alignment of SMO2-related homologues. Arabidopsis SMO2 and SMO2L and TRM112 homologues from other eukaryotes were aligned for amino acid similarity. The shading modes represent different levels of amino acid conservation, and asterisks refer to the Cys residues for zinc binding in yeast TRM112. At, *Arabidopsis thaliana*; Os, *Oryza sativa*; Hs, *Homo sapiens*; Mm, *Mus musculus*; Dm, *Drosophila melanogaster*; Ce, *Caenorhabditis elegans*; Sc, *Saccharomyces cerevisiae*.

(a)
(b)
(c)
(d)
(e)
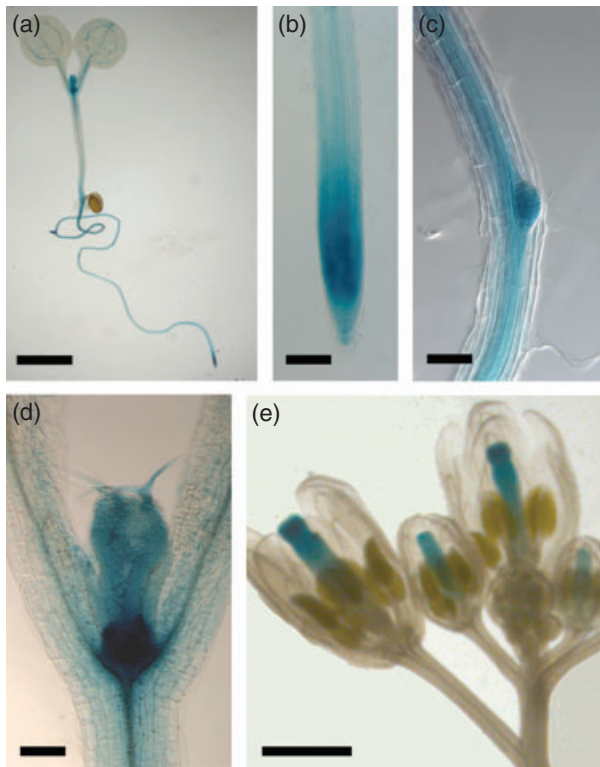
Figure 6. Tissue-specific expression of the *SMO2* gene.
GUS staining was assayed with transgenic plants expressing the *pSMO2*:GUS fusion gene in a 7-day-old seedling (a), root meristem (b), root vasculature and lateral root primordia (c), leaf primordia and juvenile leaves (d), and young siliques (e). Scale bars: 5 mm in (a); 100 μm in (b)–(d); 1 mm in (e).

identity to TRM112 homologues (Figure 5c), implying that TRM112 is an evolutionarily conserved protein. However, the putative zinc-binding domain of TRM112s in yeast, bacteria and some archaea was not present in multicellular organisms (Heurgué-Hamard *et al.*, 2006) (Figure 5c).

Yeast TRM112 has been suggested to be a multifunctional cofactor that interacts with methyltransferases and other proteins, and disruption of the *TRM112* gene in yeast resulted in a slow growth phenotype (Purushothaman *et al.*, 2005). To investigate the functional relationship between SMO2 and TRM112, we conducted a functional complementation test by expressing *SMO2* in yeast *trm112* cells. The haploid *trm112* mutant cells were isolated by sporulation of *S. cerevisiae* Y25421 and transformed with Arabidopsis *SMO2*. As shown in Figure 7(a) and (b), the slow growth phenotype resulting from impeded cell division in *trm112* cells was restored when transformed with either *SMO2* or *TRM112*, whereas *trm112* cells alone or transformed with an empty vector still grew very slowly, demonstrating that *SMO2* is a functional homologue of *TRM112*. Nevertheless, introduction of *SMO2L* into *trm112* cells just partially restored the growth of *trm112* cells (Figure S1c), further supporting the conclusion that *SMO2* and *SMO2L* have functionally diverged.

SMO2 does not affect nuclear endoreduplication in leaf cells

To substantiate the role of *SMO2* in G₂–M phase progression and investigate whether the mutation of *SMO2* affects cell endoreduplication, which is often, but not always, correlated
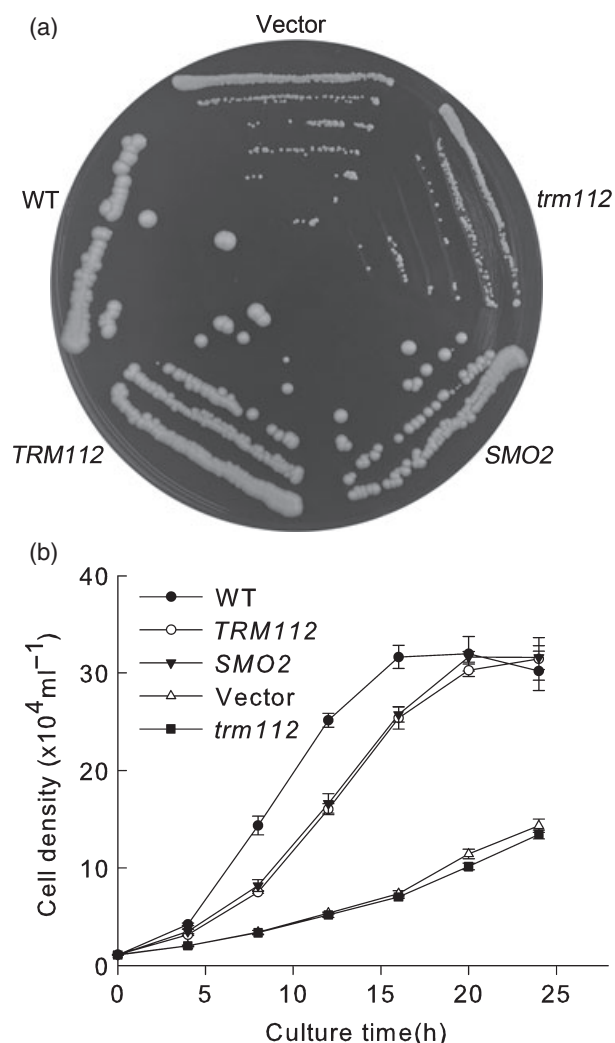
(a) Vector

WT

TRM112

trm112

SMO2

(b)

Figure 7. SMO2 is a functional homologue of yeast TRM112 protein.
(a) Functional complementation of *trm112* cells by expressing *SMO2*. Haploid *Saccharomyces cerevisiae* (wild type, WT), haploid yeast *trm112* cells (*trm112*), haploid yeast *trm112* cells carrying yeast *TRM112* (*TRM112*), *SMO2* (*SMO2*) or empty pYES2 vector (Vector) was incubated at 30°C for 3 days.
(b) Time course of yeast cell growth. The yeast cells of each genotype described above were cultured for 24 h and then diluted to OD600 = 0.15–0.17 in liquid medium as the starting concentration, and cell density was thereafter measured at intervals of 4 h. Data shown are from three biological replicates.

(a)

(b)

Figure 8. Nuclear polyploidization analysis of *smo2* leaf cells.
The juvenile (4 days after initiation) (a) and fully expanded (b) blades of fifth leaves of wild type (WT) and *smo2* plants were used for examining the cell nuclear ploidy with a flow cytometer. The percentages of cells with different nuclear polyploidy levels were calculated based on four independent replicates of each genotype and shown as averages $\pm$ SD.

with the final size of a cell (Sugimoto-Shirasu and Roberts, 2003; Ferjani *et al.*, 2007), we performed a flow cytometric examination with nuclei of both juvenile and fully expanded fifth leaves. In juvenile leaves (4 days after initiation), the percentage of 4C cells in *smo2* was indeed higher than that in WT, whereas the number of 2C cells in *smo2* was reduced accordingly (Figure 8a), further supporting that SMO2 affects G_2–M phase progression in cell cycles. In fully expanded leaves, however, *smo2* seemed to have slightly more 2C cells than WT, and the percentages of cells from 4C to 16C between two genotypes remained comparably simi-
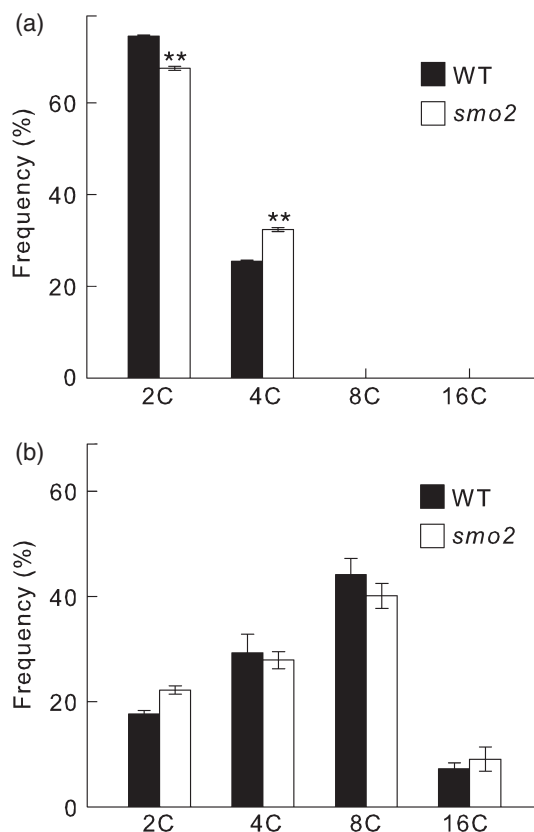
lar (Figure 8b), indicating that *smo2* does not affect nuclear DNA endoreduplication in leaf cells. Given that palisade cells in fully expanded *smo2* leaves were dramatically enlarged (Figure 2a,b), our finding also demonstrates that polyploidization is not responsible for the compensatory enlargement in *smo2* palisade cells.

DISCUSSION

SMO2 is required for the progression of cell division during organ growth

By genetic screening, we identified the *smo2* mutant with small organs and short roots, and our further analysis demonstrates that SMO2 is required for proper progression of cell division. *SMO2* is highly expressed in root and shoot meristems and the developing organs (Figure 6), and disruption of *SMO2* reduces the rate of cell production (Figure 3), thus leading to the organ growth defect. Previous studies have shown that overexpression of a non-degradable CYCB1;1 or inhibition of CYCB1;1 degradation impedes cell cycle progression in G_2 and M phases (Weingartner

et al., 2004; Pérez-Pérez *et al.*, 2008). Our findings of dramatic accumulation of CYCB1;1 in *smo2* suggest that the mutation of *SMO2* may mainly block G_2–M phase progression in the cell cycle (Figure 4), which is further supported by our observation that *smo2* juvenile leaves contain more 4C cells. On the other hand, the elevated expression of other cell cycle checkpoint genes in *smo2*, such as *CYCD3;1*, *HISTONE H4*, suggests that SMO2 is also likely to affect other cell cycle phases. In Arabidopsis, similar cell division progression defects have been reported in the mutants that mainly involve the chromatin modification or DNA repair and replication, such as *abo4-1*, *tebs* and *fas1* (Inagaki *et al.*, 2006; Ramirez-Parra and Gutierrez, 2007; Yin *et al.*, 2009). Our characterization of *smo2* provides the evidence that SMO2-mediated events are required for proper progression of cell division during plant organ growth.

Regulation of cell cycle progression and control of plant organ size

During organogenesis, proper cell cycle progression is essential for the development of an organ. In plants, retardation of the cell cycle often results in a reduction in organ size (De Veylder *et al.*, 2001; Inagaki *et al.*, 2006; Fleury *et al.*, 2007; Ramirez-Parra and Gutierrez, 2007), whereas acceleration of cell cycle progression does not appear to impinge on the final size of organs. For example, ectopic expression of *CYCD2;1* in tobacco accelerates the rate of cell production by shortening the duration of the cell cycle but does not change the final size of aerial organs (Cockcroft *et al.*, 2000), suggesting that the mechanism governing organ size by cell proliferation is beyond the control of cell cycle progression. Moreover, recent characterization of the genes involved in control of organ size, such as *AINTEGUMENTA* (*ANT*), *ARGOS*, *ARF2*, *KLUH* and *AN3* (Mizukami and Fischer, 2000; Hu *et al.*, 2003; Horiguchi *et al.*, 2005; Schruff *et al.*, 2006; Anastasiou *et al.*, 2007), strongly suggests that the duration of cell proliferation during organogenesis may be an important mechanism determining final organ size (Anastasiou and Lenhard, 2007; Gonzalez *et al.*, 2009; Krizek, 2009). Our observation that *smo2* does not affect the timing of cell proliferation suggests that SMO2 may not be a regulator of plant organ size. Indeed, overexpression of *SMO2* in Arabidopsis did not increase the final size of aerial organs (Figure S1d,e), and the reduction of leaf size in *smo2* was found to be genetically independent of those in *ant*, *35S-ARGOS*, *arf2* and *kluh* (data not shown).

Potential mechanisms by which SMO2 regulates cell division

Our finding demonstrates that Arabidopsis SMO2 is a homologue of yeast TRM112 and has a function in regulation of the progression of cell division. However, the molecular mechanism underlying such regulation is still unclear. In yeast, TRM112 has been identified as a multi-functional cofactor of tRNA and protein methyltransferases, which play roles in modification of tRNA and eRF1 (Purushothaman *et al.*, 2005; Heurgué-Hamard *et al.*, 2006; Studte *et al.*, 2008). Disruption of the *TRM112* gene leads to the defect in tRNA methylation and slows yeast cell division, but how TRM112 affects cell division remains unknown. Firstly, although a mutation in TRM11 or TRM9, a catalytic subunit of tRNA methyltransferase that interacts with TRM112, does not impede yeast growth under standard laboratory conditions (Purushothaman *et al.*, 2005; Studte *et al.*, 2008), there is no evidence that abolition of modification of both of them at tRNAs could alter yeast cell division. Secondly, TRM112 can interact with Ydr140w, a component of eRF1 methyltransferase, and disruption of Ydr140w in yeast leads to a growth defect (Niewmierzycka and Clarke, 1999; Heurgué-Hamard *et al.*, 2005, 2006), implying that TRM112 might regulate cell division through the modification of eRF1. Moreover, TRM112 is also likely to interact with other proteins, such as LYS9, SFH1 or ECM16 (Krogan *et al.*, 2006; Yu *et al.*, 2008); the possibility could not be excluded that the function of TRM112 in cell division may be via the involvement of other biological processes.

A BLAST search in Arabidopsis genome annotation has found that there exist homologues of yeast TRM9, TRM11, Ydr140w and LYS9 (data not shown), suggesting that SMO2 also potentially interacts with multiple proteins in Arabidopsis. Previous study shows that an Arabidopsis knockout mutant of LKR/SDH, a homologue of yeast LYS9, displays a phenotype indistinguishable from WT under normal growth conditions (Zhu *et al.*, 2001). However, there is still a lack of biochemical or genetic evidence about whether SMO2 interacts with these candidate partners as does the yeast homologue. Therefore, further biochemical and genetic studies on SMO2-interacting proteins in Arabidopsis are necessary to distinguish which of the interactions is responsible for the role of SMO2 in cell cycle progression during organ growth.

Functional divergence of SMO2 and SMO2L

In Arabidopsis, *SMO2L* is identified as the only gene homologous to *SMO2*. Because SMO2 and SMO2L share 78% amino acid identity and have a similar gene structure (without the intron), it is likely that *SMO2* and *SMO2L* are a result of a gene duplication event. The topology of the phylogenetic tree of TRM112 homologues from a few model organisms suggests that flowering plants and animals may have had a single ancestor *TRM112* gene, and the gene duplication events might have taken place after the splits of these species (Figure S2). Consistently, monocot rice and sorghum as well as eudicot wine grape genomes still contain a single-copy *TRM112* homologous gene, and low copy number *TRM112* homologues are found in the genomes of other plant and animal species (Figure S2).

Our findings that Arabidopsis *SMO2* is a homologue of yeast *TRM112* and *SMO2L* is not functionally redundant to *SMO2* imply that these two genes have undergone evolutionary sub/neo-functionalization. *SMO2* may retain the ancestral function of *TRM112*, because the disruption of *SMO2* alone causes retardation of the progression of cell division and *SMO2* could complement the cell division defect in yeast *trm112* cells. *SMO2L*, on the other hand, only partially rescued yeast *trm112* cells and could not complement the phenotype of *smo2* even under the *SMO2* promoter, consistent with the notion that *SMO2L* has functionally diverged from *TRM112* and *SMO2*. Although the function of *SMO2L* is unknown, our characterization of *SMO2* and *SMO2L* here illustrates that the duplicated copies of genes are functionally diversified in plants.

EXPERIMENTAL PROCEDURES

Plant materials and growth conditions

smo2 was isolated from a T-DNA transgenic population in the Columbia-0 background. Unless described otherwise, the sterilized seeds were geminated on 1/2 MS medium and all plants were grown in a culture room or growth chamber at $22 \pm 1°C$ with illumination of 80–90 μmol m^{-2} sec^{-1} and a 16-h light/8-h dark photoperiod (Jing *et al.*, 2009). For measurement of hypocotyl length, seedlings were grown vertically in the dark for 5 days.

Morphological and cytological analyses

To determine the size of leaf and palisade cells, fully expanded leaves were excised and photographed, and then cleared with chloral hydrate as previously described (Jing *et al.*, 2009). The palisade cells at approximately the central position of a half leaf were visualized under a microscope and photographed. The average cell number per area was calculated. Areas of leaves and cells were measured with IMAGE J software (http://rsbweb.nih.gov/ij/), and the total number of palisade cells per leaf was estimated by the total leaf area multiplied by the average cell number per area.

Growth kinematics and cell production in leaf and root

Growth kinematic analysis of first leaves was performed as described (De Veylder *et al.*, 2001). At least four plants of WT and *smo2* grown in the same plate were harvested daily after the first leaf initiation (when the area reached 0.02–0.03 μm^2), placed in methanol overnight, and subsequently cleared with and stored in lactic acid for microscopy. Leaf area, cell area and abaxial epidermal cell number were examined as described (De Veylder *et al.*, 2001), and an average cell division rate was determined as the slope of the log$_2$-transformed number of cells per leaf with second-degree and five-point differentiation formulae (Erickson, 1976).

For kinematic analysis of root growth, at least eight seedlings grown vertically were used for measurements of primary root length, cortex cell length and meristem size. The cell length in the mature zone and the number of cortex cells in the RM were determined with cleared primary roots under a microscope. The rate of cell production of primary root was calculated by the increased root length per day divided by the cortex cell length in the mature zone.

Flow cytometric assay

The juvenile (4 days after initiation) and fully expanded (25 days after initiation) fifth leaves of WT and *smo2* were chopped with a razor, suspended in cold nuclear isolation buffer (Galbraith *et al.*, 1983) and flow cytometric analysis was carried out as described (Jing *et al.*, 2009) with a FACS Caliber flow cytometer (BD Biosciences, http://www.bdbiosciences.com/).

Molecular cloning of *SMO2*

The flanking genomic sequence of T-DNA in *smo2* was determined by TAIL-PCR (Liu *et al.*, 1995). For *SMO2* genomic complementation, a ~2.5-kb fragment of WT genomic DNA containing a promoter and the genomic region of *SMO2* was cloned into pCAMBIA1300 and introduced into the *smo2* mutant. Meanwhile, a fusion DNA fragment of *SMO2* promoter and *SMO2L* genomic DNA in pCAMBIA 1300 was also transformed into *smo2* to investigate whether *SMO2L* is functionally equivalent to *SMO2*. In addition, the *SMO2* cDNA was cloned into pVIP96 to generate transgenic plants overexpressing *SMO2* (Hu *et al.*, 2003).

Gene expression analysis

Total RNA was isolated from 10-day-old seedlings using a guanidine thiocyanate extraction buffer (Hu *et al.*, 2000). Real-time quantitative RT-PCR (qRT-PCR) was performed with a Rotor-Gene 3000 thermocycler (Corbett Research, http://www.corbettlife-science.com/) with the SYBR® Premix Ex Taq® II kit (Takara, http://www.takara-bio.com/). The expression level of each gene was normalized against the expression levels of *ACTIN2*. The relative expression values were calculated from three biological replicates using a modified $2^{-\Delta\Delta C}T$ method (Livak and Schmittgen, 2001). The primers used for *HISTONE H4*, *CYCD3;1*, *CYCA1;1*, *CYCB2;3* and *CYCB1;1* were as described previously (Menges *et al.*, 2006; De Schutter *et al.*, 2007), and *ACTIN2* was 5'-GCTCCTCTTAACC-CAAAGGC-3' and 5'-CACACCATCACCAGAATCCAGC-3'. To examine the progression of cell division, the transgenic plant carrying *pCYCB1;1:Dbox-GUS* was crossed with *smo2*, and homozygous plants in the *smo2* background were assayed for GUS staining (Colón-Carmona *et al.*, 1999).

To investigate the tissue-specific expression of *SMO2* and *SMO2L*, a 1.8-kb *SMO2* promoter fragment and a 217-bp 3'-untranslated region of *SMO2* were fused with the β-*glucuronidase* (GUS) gene into pBI101, and a 2.0-kb promoter region of *SMO2L* was fused with GUS accordingly, to generate transgenic plants. For the GUS staining assay, seedlings or organs of homozygous transgenic plants were incubated in a 50 mM Na-phosphate solution (pH 7.0) containing 5 mM $K_4Fe(CN)_6$, 5 mM $K_3Fe(CN)_6$, 0.1% Triton X-100, and 1 mM 5-bromo-4-chloro-3-indolyl-β-glucuronic acid (Gluc) at 37°C for several hours (Hu *et al.*, 2003).

Yeast complementation

The *S. cerevisiae trm112* heterozygous mutant Y25421 (BY4743; Mat a/α; his3Δ1/his3Δ1; leu2Δ0/leu2Δ0; lys2Δ0/LYS2; MET15/met15Δ0; ura3Δ0/ura3Δ0; YNR046w::kanMX4/YNR046w) was obtained from the European *Saccharomyces Cerevisiae* Archive for Functional Analysis (EUROSCARF; Frankfurt/Main, Germany). The cells were sporulated according to the method described at the *Saccharomyces* Genome Deletion Project web page (http://www.sequence.stanford.edu/group/yeast_deletion_project/spo_riles), and subsequently digested by 1% nailase for 90 min. The digested spores were diluted to 1:10^7 and spotted on yeast peptone dextrose (YPD) medium for 4 days at 30°C and individual colonies were identified by PCR for haploid *trm112* and *TRM112* cells. The cDNA fragments of *SMO2*, *SMO2L* and yeast *TRM112* were cloned to pYES2 and introduced into *trm112* cells, respectively. The yeast transformation and culture were performed according to standard protocols (Gietz and Woods, 2002). The yeast cells of each genotype

were diluted to OD600 = 0.15–0.17 in liquid medium, and the cell density was determined at intervals of 4 h.

Sequence alignment and phylogenetic tree construction

All *SMO2* homologues were identified from GenBank using the protein basic local alignment search tool (BLASTp) (http://blast.ncbi.nlm.nih.gov/Blast.cgi). The alignment of full-length amino acid sequences was used to construct the neighbour-joining (NJ) tree using the MEGA3 (Molecular Evolutionary Genetic Analyses, version1.1, Pennsylvania State University, http://www.megasoftware.net/) package. The boot strap values were calculated using 1000 replicates (Lü *et al.*, 2007).

SUPPORTING INFORMATION

Additional Supporting Information may be found in the online version of this article:
Figure S1. Functional characterization of *SMO2* and *SMO2L.*
Figure S2. Phylogenetic tree of *SMO2* homologues.
Please note: As a service to our authors and readers, this journal provides supporting information supplied by the authors. Such materials are peer-reviewed and may be re-organized for online delivery, but are not copy-edited or typeset. Technical support issues arising from supporting information (other than missing files) should be addressed to the authors.

REFERENCES

Achard, P., Gusti, A., Cheminant, S., Alioua, M., Dhondt, S., Coppens, F., Beemster, G.T. and Genschik, P. (2009) Gibberellin signaling controls cell proliferation rate in *Arabidopsis. Curr. Biol.* **19**, 1188–1193.

Anastasiou, E. and Lenhard, M. (2007) Growing up to one's standard. *Curr. Opin. Plant Biol.* **10**, 63–69.

Anastasiou, E., Kenz, S., Gerstung, M., MacLean, D., Timmer, J., Fleck, C. and Lenhard, M. (2007) Control of plant organ size by *KLUH/CYP78A5*-dependent intercellular signaling. *Dev. Cell,* **13**, 843–856.

Andersen, S.U., Buechel, S., Zhao, Z., Ljung, K., Novák, O., Busch, W., Schuster, C. and Lohmann, J.U. (2008) Requirement of B2-type *Cyclin-Dependent Kinases* for meristem integrity in *Arabidopsis thaliana. Plant Cell,* **20**, 88–100.

Baskin, T.I. (2000) On the constancy of cell division rate in the root meristem. *Plant Mol. Biol.* **43**, 545–554.

Beemster, G.T. and Baskin, T.I. (1998) Analysis of cell division and elongation underlying the developmental acceleration of root growth in *Arabidopsis thaliana. Plant Physiol.* **116**, 1515–1526.

Beemster, G.T., Fiorani, F. and Inzé, D. (2003) Cell cycle: the key to plant growth control? *Trends Plant Sci.* **8**, 154–158.

Blilou, I., Frugier, F., Folmer, S., Serralbo, O., Willemsen, V., Wolkenfelt, H., Eloy, N.B., Ferreira, P.C., Weisbeek, P. and Scheres, B. (2002) The *Arabidopsis HOBBIT* gene encodes a CDC27 homolog that links the plant cell cycle to progression of cell differentiation. *Genes Dev.* **16**, 2566–2575.

Cockcroft, C.E., den Boer, B.G., Healy, J.M. and Murray, J.A. (2000) Cyclin D control of growth rate in plants. *Nature,* **405**, 575–579.

Colón-Carmona, A., You, R., Haimovitch-Gal, T. and Doerner, P. (1999) Spatio-temporal analysis of mitotic activity with a labile cyclin-GUS fusion protein. *Plant J.* **20**, 503–508.

Criqui, M.C., Weingartner, M., Capron, A., Parmentier, Y., Shen, W.H., Heberle-Bors, E., Bögre, L. and Genschik, P. (2001) Sub-cellular localization of GFP-tagged tobacco mitotic cyclins during the cell cycle and after spindle checkpoint activation. *Plant J.* **28**, 569–581.

Da Costa, M., Bach, L., Landrieu, I., Bellec, Y., Catrice, O., Brown, S., De Veylder, L., Lippens, G., Inzé, D. and Faure, J.D. (2006) *Arabidopsis* PASTICCINO2 is an antiphosphatase involved in regulation of cyclin-dependent kinase A. *Plant Cell,* **18**, 1426–1437.

De Schutter, K., Joubès, J., Cools, T. *et al.* (2007) *Arabidopsis* WEE1 kinase controls cell cycle arrest in response to activation of the DNA integrity checkpoint. *Plant Cell,* **19**, 211–225.

De Veylder, L., Beeckman, T., Beemster, G.T., Krols, L., Terras, F., Landrieu, I., van der Schueren, E., Maes, S., Naudts, M. and Inzé, D. (2001) Functional analysis of cyclin-dependent kinase inhibitors of Arabidopsis. *Plant Cell,* **13**, 1653–1668.

De Veylder, L., Beeckman, T., Beemster, G.T. *et al.* (2002) Control of proliferation, endoreduplication and differentiation by the *Arabidopsis* E2Fa-DPa transcription factor. *EMBO J.* **21**, 1360–1368.

De Veylder, L., Beeckman, T. and Inzé, D. (2007) The ins and outs of the plant cell cycle. *Nat. Rev. Mol. Cell Biol.* **8**, 655–665.

Desvoyes, B., Ramirez-Parra, E., Xie, Q., Chua, N.H. and Gutierrez, C. (2006) Cell type-specific role of the retinoblastoma/E2F pathway during Arabidopsis leaf development. *Plant Physiol.* **140**, 67–80.

Dewitte, W. and Murray, J.A. (2003) The plant cell cycle. *Annu. Rev. Plant Biol.* **54**, 235–264.

Dewitte, W., Scofield, S., Alcasabas, A.A. *et al.* (2007) *Arabidopsis* CYCD3 D-type cyclins link cell proliferation and endocycles and are rate-limiting for cytokinin responses. *Proc. Natl Acad. Sci. USA,* **104**, 14537–14542.

Dohmann, E.M., Levesque, M.P., De Veylder, L., Reichardt, I., Jürgens, G., Schmid, M. and Schwechheimer, C. (2008) The *Arabidopsis* COP9 signalosome is essential for G2 phase progression and genomic stability. *Development,* **135**, 2013–2022.

Erickson, R.O. (1976) Modeling of plant growth. *Annu. Rev. Plant Physiol.* **27**, 407–434.

Ferjani, A., Horiguchi, G., Yano, S. and Tsukaya, H. (2007) Analysis of leaf development in *fugu* mutants of Arabidopsis reveals three compensation modes that modulate cell expansion in determinate organs. *Plant Physiol.* **144**, 988–999.

Figaro, S., Scrima, N., Buckingham, R.H. and Heurgué-Hamard, V. (2008) HemK2 protein, encoded on human chromosome 21, methylates translation termination factor eRF1. *FEBS Lett.* **582**, 2352–2356.

Fleury, D., Himanen, K., Cnops, G. *et al.* (2007) The *Arabidopsis thaliana* homolog of yeast *BRE1* has a function in cell cycle regulation during early leaf and root growth. *Plant Cell,* **19**, 417–432.

Galbraith, D.W., Harkins, K.R., Maddox, J.M., Ayres, N.M., Sharma, D.P. and Firoozabady, E. (1983) Rapid flow cytometric analysis of the cell cycle in intact plant tissues. *Science,* **220**, 1049–1051.

Gietz, R.D. and Woods, R.A. (2002) Transformation of yeast by lithium acetate/single-stranded carrier DNA/polyethylene glycol method. *Methods Enzymol.* **350**, 87–96.

Gonzalez, N., Beemster, G.T. and Inzé, D. (2009) David and Goliath: what can the tiny weed *Arabidopsis* teach us to improve biomass production in crops? *Curr. Opin. Plant Biol.* **12**, 157–164.

Gutierrez, C. (2009) The Arabidopsis cell division cycle. In *The Arabidopsis Book* (Somerville, C.R. and Meyerowitz, E.M. eds). Rockville, MD: American Society of Plant Biologists. doi:10.1199/tab.0120, http://www.aspb.org/publications/arabidopsis.

Heurgué-Hamard, V., Champ, S., Mora, L., Merkulova-Rainon, T., Kisselev, L.L. and Buckingham, R.H. (2005) The glutamine residue of the conserved GGQ motif in *Saccharomyces cerevisiae* release factor eRF1 is methylated by the product of the *YDR140w* gene. *J. Biol. Chem.* **280**, 2439–2445.

Heurgué-Hamard, V., Graille, M., Scrima, N., Ulryck, N., Champ, S., van Tilbeurgh, H. and Buckingham, R.H. (2006) The zinc finger protein Ynr046w is plurifunctional and a component of the eRF1 methyltransferase in yeast. *J. Biol. Chem.* **281**, 36140–36148.

Horiguchi, G., Kim, G.T. and Tsukaya, H. (2005) The transcription factor AtGRF5 and the transcription coactivator AN3 regulate cell proliferation in leaf primordia of *Arabidopsis thaliana. Plant J.* **43**, 68–78.

Hu, Y., Bao, F. and Li, J. (2000) Promotive effect of brassinosteroids on cell division involves a distinct *CycD3*-induction pathway in *Arabidopsis*. *Plant J.* **24**, 693–701.

Hu, Y., Xie, Q. and Chua, N.H. (2003) The Arabidopsis auxin-inducible gene *ARGOS* controls lateral organ size. *Plant Cell*, **15**, 1951–1961.

Inagaki, S., Suzuki, T., Ohto, M.A., Urawa, H., Horiuchi, T., Nakamura, K. and Morikami, A. (2006) *Arabidopsis* TEBICHI, with helicase and DNA polymerase domains, is required for regulated cell division and differentiation in meristems. *Plant Cell*, **18**, 879–892.

Ingram, G.C. and Waites, R. (2006) Keeping it together: co-ordinating plant growth. *Curr. Opin. Plant Biol.* **9**, 12–20.

Inzé, D. and De Veylder, L. (2006) Cell cycle regulation in plant development. *Annu. Rev. Genet.* **40**, 77–105.

Ivanov, V.B., Dobrochaev, A.E. and Baskin, T.I. (2002) What the distribution of cell lengths in the root meristem does and does not reveal about cell division. *J. Plant Growth Regul.* **21**, 60–67.

Jing, Y., Cui, D., Bao, F., Hu, Z., Qin, Z. and Hu, Y. (2009) Tryptophan deficiency affects organ growth by retarding cell expansion in Arabidopsis. *Plant J.* **57**, 511–521.

Kaya, H., Shibahara, K.I., Taoka, K.I., Iwabuchi, M., Stillman, B. and Araki, T. (2001) *FASCIATA* genes for chromatin assembly factor-1 in *Arabidopsis* maintain the cellular organization of apical meristems. *Cell*, **104**, 131–142.

Krizek, B.A. (2009) Making bigger plants: key regulators of final organ size. *Curr. Opin. Plant Biol.* **12**, 17–22.

Krogan, N.J., Cagney, G., Yu, H. et al. (2006) Global landscape of protein complexes in the yeast *Saccharomyces cerevisiae*. *Nature*, **440**, 637–643.

Liu, Y.G., Mitsukawa, N., Oosumi, T. and Whittier, R.F. (1995) Efficient isolation and mapping of *Arabidopsis thaliana* T-DNA insert junctions by thermal asymmetric interlaced PCR. *Plant J.* **8**, 457–463.

Livak, K.J. and Schmittgen, T.D. (2001) Analysis of relative gene expression data using real-time quantitative PCR and the $2^{-\Delta\Delta C}T$ method. *Methods*, **25**, 402–408.

Lü, S., Du, X., Lu, W., Chong, K. and Meng, Z. (2007) Two *AGAMOUS*-like MADS-box genes from *Taihangia rupestris* (Rosaceae) reveal independent trajectories in the evolution of class C and class D floral homeotic functions. *Evol. Dev.* **9**, 92–104.

Malumbres, M. (2005) Revisiting the ''Cdk-centric'' view of the mammalian cell cycle. *Cell Cycle*, **4**, 206–210.

Menges, M., Samland, A.K., Planchais, S. and Murray, J.A. (2006) The D-type cyclin CYCD3;1 is limiting for the G1-to-S-phase transition in *Arabidopsis*. *Plant Cell*, **18**, 893–906.

Mizukami, Y. (2001) A matter of size: developmental control of organ size in plants. *Curr. Opin. Plant Biol.* **4**, 533–539.

Mizukami, Y. and Fischer, R.L. (2000) Plant organ size control: *AINTEGUMENTA* regulates growth and cell numbers during organogenesis. *Proc. Natl Acad. Sci. USA*, **97**, 942–947.

Niewmierzycka, A. and Clarke, S. (1999) *S*-Adenosylmethionine-dependent methylation in *Saccharomyces cerevisiae*. Identification of a novel protein arginine methyltransferase. *J. Biol. Chem.* **274**, 814–824.

Pérez-Pérez, J.M., Serralbo, O., Vanstraelen, M., González, C., Criqui, M.C., Genschik, P., Kondorosi, E. and Scheres, B. (2008) Specialization of CDC27 function in the Arabidopsis thaliana anaphase-promoting complex (APC/C). *Plant J.* **53**, 78–89.

del Pozo, J.C., Lopez-Matas, M.A., Ramirez-Parra, E. and Gutierrez, C. (2005) Hormonal control of the plant cell cycle. *Physiol. Plant.* **123**, 173–183.

del Pozo, J.C., Diaz-Trivino, S., Cisneros, N. and Gutierrez, C. (2006) The balance between cell division and endoreplication depends on E2FC-DPB,
transcription factors regulated by the ubiquitin-SCF^{SKP2A} pathway in *Arabidopsis*. *Plant Cell*, **18**, 2224–2235.

Purushothaman, S.K., Bujnicki, J.M., Grosjean, H. and Lapeyre, B. (2005) Trm11p and Trm112p are both required for the formation of 2-methylguanosine at position 10 in yeast tRNA. *Mol. Cell. Biol.* **25**, 4359–4370.

Ramirez-Parra, E. and Gutierrez, C. (2007) E2F regulates *FASCIATA1*, a chromatin assembly gene whose loss switches on the endocycle and activates gene expression by changing the epigenetic status. *Plant Physiol.* **144**, 105–120.

Scheres, B. and Wolkenfelt, H. (1998) The *Arabidopsis* root as a model to study plant development. *Plant Physiol. Biochem.* **36**, 21–32.

Schruff, M.C., Spielman, M., Tiwari, S., Adams, S., Fenby, N. and Scott, R.J. (2006) The *AUXIN RESPONSE FACTOR 2* gene of *Arabidopsis* links auxin signalling, cell division, and the size of seeds and other organs. *Development*, **133**, 251–261.

Studte, P., Zink, S., Jablonowski, D., Bär, C., von der Haar, T., Tuite, M.F. and Schaffrath, R. (2008) tRNA and protein methylase complexes mediate zymocin toxicity in yeast. *Mol. Microbiol.* **69**, 1266–1277.

Sugimoto-Shirasu, K. and Roberts, K. (2003) ''Big it up'': endoreduplication and cell-size control in plants. *Curr. Opin. Plant Biol.* **6**, 544–553.

Takatsuka, H., Ohno, R. and Umeda, M. (2009) The Arabidopsis cyclin-dependent kinase-activating kinase CDKF;1 is a major regulator of cell proliferation and cell expansion but is dispensable for CDKA activation. *Plant J.* **59**, 475–487.

Tsukaya, H. (2003) Organ shape and size: a lesson from studies of leaf morphogenesis. *Curr. Opin. Plant Biol.* **6**, 57–62.

Tsukaya, H. (2006) Mechanism of leaf-shape determination. *Annu. Rev. Plant Biol.* **57**, 477–496.

Tsukaya, H. (2008) Controlling size in multicellular organs: focus on the leaf. *PLoS Biol.* **6**, e174.

Ubeda-Tomás, S., Federici, F., Casimiro, I., Beemster, G.T., Bhalerao, R., Swarup, R., Doerner, P., Haseloff, J. and Bennett, M.J. (2009) Gibberellin signaling in the endodermis controls *Arabidopsis* root meristem size. *Curr. Biol.* **19**, 1194–1199.

Wang, H., Zhou, Y., Gilmer, S., Whitwill, S. and Fowke, L.C. (2000) Expression of the plant cyclin-dependent kinase inhibitor ICK1 affects cell division, plant growth and morphology. *Plant J.* **24**, 613–623.

Weingartner, M., Criqui, M.C., Mészáros, T., Binarova, P., Schmit, A.C., Helfer, A., Derevier, A., Erhardt, M., Bögre, L. and Genschik, P. (2004) Expression of a nondegradable cyclin B1 affects plant development and leads to endomitosis by inhibiting the formation of a phragmoplast. *Plant Cell*, **16**, 643–657.

Willemsen, V., Wolkenfelt, H., de Vrieze, G., Weisbeek, P. and Scheres, B. (1998) The *HOBBIT* gene is required for formation of the root meristem in the *Arabidopsis* embryo. *Development*, **125**, 521–531.

Yin, H., Zhang, X., Liu, J., Wang, Y., He, J., Yang, T., Hong, X., Yang, Q. and Gong, Z. (2009) Epigenetic regulation, somatic homologous recombination, and abscisic acid signaling are influenced by DNA polymerase ε mutation in *Arabidopsis*. *Plant Cell*, **21**, 386–402.

Yu, H., Braun, P., Yildirim, M.A. et al. (2008) High-quality binary protein interaction map of the yeast interactome network. *Science*, **322**, 104–110.

Zhu, X., Tang, G., Granier, F., Bouchez, D. and Galili, G. (2001) A T-DNA insertion knockout of the bifunctional lysine-ketoglutarate reductase/saccharopine dehydrogenase gene elevates lysine levels in Arabidopsis seeds. *Plant Physiol.* **126**, 1539–1545.